

# Flexomagnetic effect in Mn-based antiperovskites

Pavel Lukashev and Renat F. Sabirianov\*

Department of Physics, University of Nebraska, Omaha, Nebraska 68182

(Dated: October 29, 2018)

We report appearance of the net magnetization in Mn-based antiperovskite compounds as a result of the external strain gradient (*flexomagnetic effect*). In particular, we describe the mechanism of the magnetization induction in the Mn<sub>3</sub>GaN at the atomic level in terms of the behavior of the local magnetic moments (LMM) of the Mn atoms. We show that the flexomagnetic effect is linear and results from the non-uniformity of the strain, i.e. it is absent not only in the ground state but also when the applied external strain is uniform. We estimate the flexomagnetic coefficient to be 1.95  $\mu_B \text{ \AA}$ . We show that at the moderate values of the strain gradient ( $\sim 0.1\%$ ) the flexomagnetic contribution is the only non-vanishing input to the induced magnetization.

PACS numbers:

Magneto-mechanical coupling in crystals has many practical applications, such as in sensors, magnetic recording devices, etc. The correlation between external strain and induced magnetization is in principal significant for the systems with different dimensionality, i.e. bulk, thin film, and nano configurations. Yet, the correlation between the strain gradient and induced magnetization is especially important in nanostructures and thin film heterostructures because of the large surface-to-volume ratio which may result in a large surface tension due to the structural distortions caused by lattice mismatch, external stress, etc. For example the strain gradient may play a significant role when thin film is epitaxially grown on a substrate with slightly different lattice parameters. On the other hand, in problems concerning bulk structures the strain gradient is small and as a result has only negligible contribution. This is so because of the dimensional scaling inherent in the very definition of the strain gradient, i.e. the decrease of the characteristic length of the system,  $x$  results in increase of the  $\Delta x/x$  ratio. Fig. 1 schematically shows possible geometries of the systems under external strain gradient: bent nano-wire and nano-pill grown on a substrate. The "in-plane" and "out-of-plane" orientations of the induced magnetization shown on Fig. 1 will be explained later in the text.

The magneto-mechanical coupling is phenomenologically described by adding additional terms to the expression for the thermodynamic potential, i.e. free energy, proportional to the product of the magnetic field component and the conjugate terms involving mechanical strain:

$$F_{magn} = -\lambda_{i,jk} H_i \sigma_{jk} - \mu_{i,jk} H_i \sigma_{jk}^2 - \nu_{ijkl} H_i \frac{\partial \sigma_{jk}}{\partial x_l};$$

$$i, j, k, l = 1, 2, 3 \quad (1)$$

where  $\lambda_{i,jk}$  is the piezomagnetic tensor,  $H_i$  is the  $i$ -th component of the magnetic field ( $i = x, y, z$ ),  $\sigma_{jk}$  is the elastic stress tensor,  $\mu_{i,jk}$  is the magneto-elastic tensor,  $\nu_{ijkl}$  is the 4-rank tensor (*flexomagnetic tensor*), and  $\frac{\partial \sigma_{jk}}{\partial x_l}$  is the strain gradient. For example, piezomagnetic (magnetostrictive) properties of certain antiferromagnetic (AFM) materials are reflected in a term linear both in the magnetic field and in the elastic stress tensor [1]. For the bulk structures the last term on the r.h.s. of (1) is usually omitted because of its negligible contribution, yet in nanostructures and/or thin film heterostructures it plays a significant role.

By taking partial derivative of (1) w.r.t. magnetic field component,  $H_i$  we get the net magnetization in the system, which may be linear w.r.t. the strain (i.e. piezomagnetic effect), quadratic (second order magneto-elastic effect), and proportional to the strain gradient:

$$M_i = \underbrace{\lambda_{i,jk} \sigma_{jk}}_{\text{piezo}} + \underbrace{\mu_{i,jk} \sigma_{jk}^2}_{\text{mag-elast}} + \underbrace{\nu_{ijkl} \frac{\partial \sigma_{jk}}{\partial x_l}}_{\text{flex}};$$

$$i, j, k, l = 1, 2, 3 \quad (2)$$

It is important to emphasize that the symmetries of the  $\lambda_{i,jk}$  and  $\mu_{i,jk}$  tensors are different from the symmetry of the  $\nu_{ijkl}$  tensor in (2), which means that the induced magnetization will have three contributions in principal distinguishable by symmetry arguments only. Moreover, it is possible that because of the crystal and magnetic symmetry the linear piezomagnetism will be absent in the system with the nonzero strain gradient induced magnetization. We define the contribution to the  $M_i$  from the third term on the r.h.s. of Eq. (2) as *flexomagnetic (FLM) effect*, i.e. strain gradient induced magnetization.

To the best of our knowledge the term *flexomagneto-electric effect* was first coined by Bobylev and Pikin in their study of the correlation between elastic and electromagnetic properties of nematic liquid crystals [2]. As a sidenote we emphasize here that in their work Bobylev and Pikin discussed the "reverse" flexomagneto-electric-

\*Also at Nebraska Center for Materials and Nanotechnology, University of Nebraska, Lincoln, Nebraska 68588

ity, i.e. the re-orientation (which they called *flex*) of the molecules under external electric and magnetic fields. Much work was done in the past to investigate the correlation between electric polarization and external strain gradient, at both experimental and theoretical level [3], [4], [5]. Yet, the correlation between magnetic behavior of the system and the gradient of the strain was not the subject of mainstream research. One of the reasons for the insufficient study on this matter is the obvious complexity of the problem, - as opposed to the flexoelectric effect, where the electric polarization directly correlates with the atomic displacements, the FIM effect is indirect, i.e. it results from the re-orientation of the atomic spins following the atomic displacements (because of the exchange interaction). As a result, for the FIM effect one has to consider not only the crystal but also the magnetic structure and symmetry. Systems of interest must satisfy certain conditions, such as they have to be non-magnetic in ground state, and at the same time they have to exhibit strong magneto-elastic coupling. Comparatively well known manifestation of these properties is the piezomagnetic effect, i.e. induction of a spontaneous magnetic moment in the system under mechanical strain. In what follows we present the results of our study of the external strain gradient induced magnetization mechanism.

To understand the mechanism of flexomagnetism at the atomic level we perform first principles study for the  $\text{Mn}_3\text{GaN}$  under strain gradient. The choice of the material is based on the intriguing magneto-mechanical coupling mechanism in  $\text{Mn}_3\text{GaN}$ . In its ground state  $\text{Mn}_3\text{GaN}$  is non-magnetic with non-collinear  $\Gamma^{5g}$  structure (in the classification of Bertaut et al. [6]), i.e. the Mn LMMs on the (111) plane form clockwise or counterclockwise configurations, such that the spin moments in the plane are compensating each other. The atoms of Mn, Ga and N form an antiperovskite (AP) crystal structure, and the lattice constant of the primitive 5-atom cell of  $\text{Mn}_3\text{GaN}$  is 3.86 Å. Fig. 2 shows the unit cell of the  $\text{Mn}_3\text{GaN}$  in the ground state.

In our recent work [7] we have shown that the application of the external stress to the Mn-based AP compounds results in appearance of the non-zero magnetic moment, i.e. these compounds exhibit *piezomagnetic* properties. This can be explained from the symmetry viewpoint, i.e. as a result of the applied biaxial strain the symmetry of the system reduces from the trigonal space group  $P\bar{3}1m$  to the orthorhombic  $Pm'm'm$  ferromagnetic space group. Because of this transition some of the symmetry operations are not compatible anymore with the new structure. The appearance of the net magnetization in the system under external stress is due to the rotation of the LMMs of the Mn atoms from their equilibrium positions. After rotation the LMMs in the (111)-plane become inequivalent and do not compensate each other anymore. The piezomagnetic effect is linear and magnetization reversal is potentially possible upon reversal of the sign of the strain (compressive to tensile or

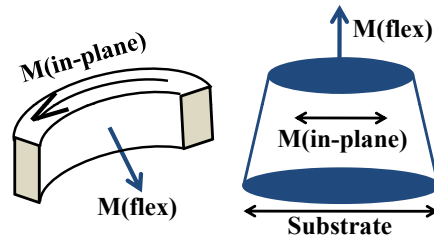


FIG. 1: Schematic picture of the systems under strain gradient with possible orientations of the induced magnetization.

vice versa). In the present work we examine the magnetic behavior of the  $\text{Mn}_3\text{GaN}$  under strain gradient (*flexure*), i.e. we look at the third term on the r.h.s. of Eq. (2).

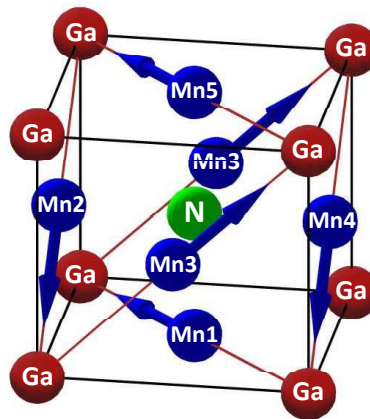


FIG. 2: (color online) Ground state of the antiperovskite  $\text{Mn}_3\text{GaN}$  unit cell: non-collinear  $\Gamma^{5g}$  magnetic structure. Local magnetic moments are shown by blue arrow on Mn atoms.

We use projector augmented wave (PAW) method by Blöchl [8], implementation of PAW by G. Kresse and D. Joubert [9] in the Vienna *ab initio* simulation package (VASP) code within a Perdew-Burke-Ernzerhof (PBE) generalized gradient approximation [10] of the density functional theory (DFT). We use a  $3 \times 12 \times 6$  k-point sampling and the Blöchl's tetrahedron integration method [11]. We set the plane-wave cut-off energy to 300 eV and we choose the convergence criteria for energy of  $10^{-5}$  eV.

Accurate electronic structure calculations require periodic boundary condition. The strain gradient breaks the periodicity of the primitive unit cell, therefore to construct a model with translational symmetry we have to take larger cell. For  $\text{Mn}_3\text{GaN}$  the smallest possible configuration to retain the translational symmetry under external strain gradient consists of the 8 primitive cells of  $\text{Mn}_3\text{GaN}$  ( $4 \times 2 \times 1$  cell configuration). To simulate the strain gradient we introduce small relative atomic

Step	Mn ( $\text{\AA}$ )	Ga ( $\text{\AA}$ )	Flex (%)
1	0.01868	0.03736	0.242
2	0.03736	0.07442	0.484
3	0.05589	0.11179	0.724
4	0.07450	0.14900	0.965
5	0.09264	0.18528	1.200
6	0.11132	0.22234	1.442

TABLE I: Atomic shifts of Mn and Ga atoms and strain gradients:  $\text{Mn}_{24}\text{Ga}_8\text{N}_8$ .

shifts of Ga and Mn atoms in a way, which splits our 40-atom cell in 4 domains (see Fig. 3, top panel). In each of the four domains we have strain gradient,  $\Delta a/a$  (schematically shown on the bottom panel of the Fig. 3), and 4-domain configuration satisfies the periodic boundary condition. The initial orientation of the LMMs forms non-collinear  $\Gamma^{5g}$  structure. In our model we have "flat" triangular LMM configuration (Fig. 3, bottom panel), while on Fig. 2 LMMs are on the (111) plane. Both magnetic orientations are energetically indistinguishable, and we pick the "flat" system for simplicity. Table I summarizes the values for the atomic shifts and the strain gradients for the  $\text{Mn}_{24}\text{Ga}_8\text{N}_8$  cell.

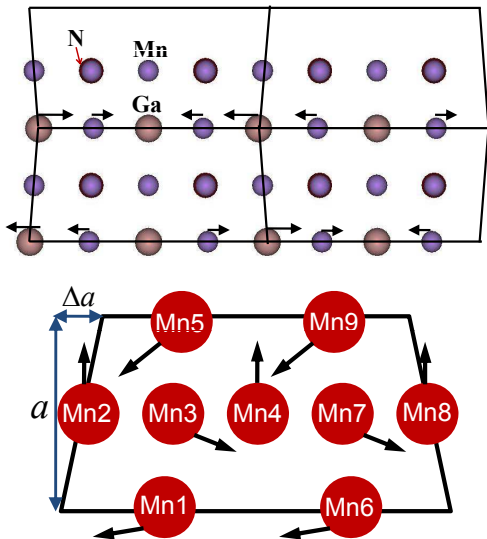


FIG. 3: (color online) Top panel:  $\text{Mn}_{24}\text{Ga}_8\text{N}_8$  cell: 4-domain structure. Mn atoms - blue, Ga atoms - grey, N atoms - dark red (almost invisible behind Mn atoms). The directions of the atomic shifts are schematically shown by black arrows. Bottom panel: Single domain in  $\text{Mn}_{24}\text{Ga}_8\text{N}_8$  under strain gradient.

Next we relax the LMMs of the Mn atoms but we keep the atomic positions fixed to make sure that the crystal structure does not relax back to the unstrained

ground state. Fig. 4 shows results of our calculations for the magnetization per Mn atom as a function of the strain gradient. There are two different contributions: the blue line with circles represents out-of-plane magnetization (multiplied by 10) which is a direct result of the flexure. If the strain applied to the cell is uniform then from the symmetry arguments it is clear that only in-plane magnetization will appear. The black line with squares represents in-plane non-linear contribution to the magnetization which results from the in-plane rotations of the LMMs of the Mn atoms (shown on the bottom panel of the Fig. 3 by black arrows). Important feature of these two mechanisms is that at the moderate values of the strain gradient the dominant contribution comes from the linear flexomagnetic magnetization, while the non-linear in-plane contribution is vanishingly small. This correlation changes at the higher values of the gradient but the dominant nature of the linear contribution at the moderate gradient values is important for the practical applications where the regular values of the strain gradient are of the order of  $\sim 0.1 \div 0.2\%$ .

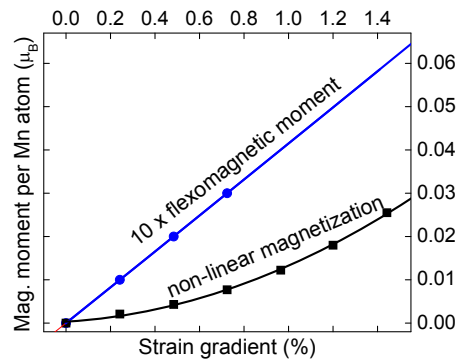


FIG. 4: (color online) Linear out-of-plane ( $\times 10$ ) and non-linear in-plane induced net magnetization of Mn atom as a function of the strain gradient.

To understand better the nature of these two contributions we examine the behavior of in-plane and out-of-plane components of the LMMs of Mn atoms within one domain. Figures 5 and 6 show our results. The out-of-plane contribution comes from the Mn atoms 3, 4 and 7 (see Fig. 3, bottom panel). At the same time the in-plane rotations of the Mn LMMs (atoms 3 and 7) show distinct non-linear feature, which contributes to the non-linear in-plane magnetization shown on Fig. 4. The appearance of the out-of-plane component is not observed if the applied strain is uniform. Therefore, the appearance of the linear out-of-plane magnetization is purely strain gradient related effect and its mechanism is different from the one responsible for the in-plane magnetization induction. Below we present our phenomenological arguments on the mechanism of the FIM effect at the atomic level and estimate the value of the FIM coefficient.

Qualitatively, the out-of-plane rotations of the LMMs

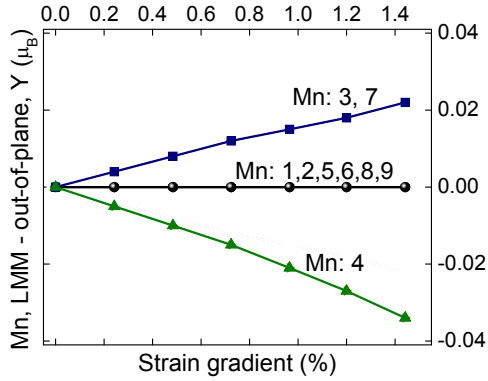


FIG. 5: Out-of-plane magnetic moment vs. strain gradient.

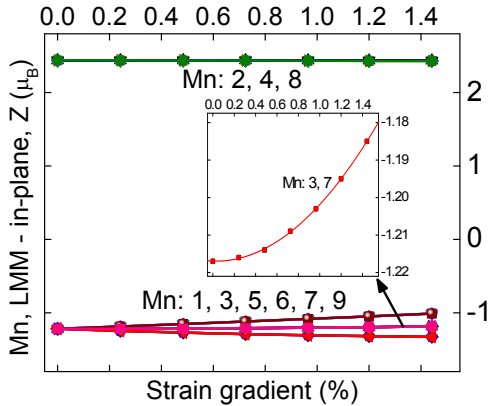


FIG. 6: In-plane magnetic moment vs. strain gradient.

can be explained by the frustration of the spin orientations. Because of the inequivalent strain on different lattice sites the ground state nearest neighbor distances between Mn atoms change in non-uniform way. This is schematically shown on the bottom panel of the Fig. 3 where for example the  $Mn1 \leftrightarrow Mn4$  distance becomes larger than the  $Mn4 \leftrightarrow Mn5$  distance. This is a

pure strain gradient related effect, this non-uniformity is not present in the ground state and in the case of the uniform strain. This results in the increase of the exchange integral,  $J(\mathbf{r}_{4,5})$  in the Heisenberg Hamiltonian between Mn4 and Mn5 atoms (see Fig. 3, bottom panel) due to the increasing overlap of their wave functions and at the same time in the decrease of the  $J(\mathbf{r}_{1,4})$  between Mn1 and Mn4 atoms. This mechanism is responsible for the out-of-plane rotation of the Mn4 (and other "inside of the domain" Mn atoms, such as Mn3 and Mn7 on the Fig. 3, bottom panel) LMM.

We estimate the flexomagnetic coefficient at the strain gradient value of  $\sim 0.4\%$  from Eq.(2) and the magnetization vs. strain gradient data shown on Fig. 4 as follows.

$$M_{flex} = \nu \frac{\partial \sigma}{\partial x};$$

$$\frac{\partial \sigma}{\partial x} = \frac{\partial}{\partial x} \left[ \frac{\Delta a_0}{a_0} \right] = \frac{\partial}{\partial x} \left[ \frac{a_0 + c \cdot x}{a_0} \right] = \frac{1}{a_0} c \approx \frac{0.004}{3.9 \cdot 10^{-10} m};$$

$$\nu = \frac{M_{flex}}{\frac{\partial \sigma}{\partial x}} = \frac{0.002 \mu_B}{0.004 / 3.9 \cdot 10^{-10} m} \Rightarrow \nu \sim 1.95 \mu_B \text{ \AA}.$$

Here  $a_0 = 3.9 \cdot 10^{-10} m$  is the ground state lattice constant of the  $Mn_3GaN$ ,  $M_{flex} = 0.002 \mu_B$  is the induced out-of-plane magnetization value at  $\sim 0.4\%$  of the strain gradient. Since the magnetization is linear, the  $\nu$  will have the same value over the considered range of the strain gradient.

In summary, in this paper we discussed the appearance of the net magnetization in Mn-based antiperovskite compounds (in particular,  $Mn_3GaN$ ) under external strain gradient (*flexomagnetic effect*). The magnetization dependance on the *flexure* is linear. The estimated flexomagnetic coefficient is  $1.95 \mu_B \text{ \AA}$ . Besides being of substantial theoretical value, the flexomagnetic effect can have interesting practical applications, such as in electrical control of magnetization in memory cells if the structural distortion in the flexomagnetic phase is induced and can be controlled by the external electric field (i.e. by forming heterostructure with ferroelectric/piezoelectric compounds).

This work was supported by the National Science Foundation and the Nanoelectronics Research Initiative through the Materials Research Science and Engineering Center at the University of Nebraska. This work was completed utilizing the Blackforest Cluster Computing Facility of the College of Information Science and Technology at University of Nebraska at Omaha.

- [1] Landau L. D., Lifshitz E. M., Pitaevskii L. P., *Electrodinamika Sploshnykh Sred (Electrodynamics of Continuous Media)*, (Moscow: FIZMATLIT), 2005.
- [2] Yu. P. Bobylev and S. A. Pikin, *Pis'ma Zh. Tekh. Fiz.* **5**, 1032-1035 (September 12, 1979). *Translated and published in English as* Yu. P. Bobylev and S. A. Pikin, *Sov. Tech. Phys. Lett.* 5(9), 430-1, September 1979.
- [3] A. K. Tagantsev, *Zh. Eksp. Teor. Fiz.* **88**, 2108-2122 (June 1985). *Translated and published in English as* A. K. Tagantsev, *Sov. Phys. JETP* **61** (6), June 1985.
- [4] V. L. Indenbom, E. B. Loginov, and M. A. Osipov,

- Kristallografiya* **26** 1157-1162 (November-December 1981). *Translated and published in English as* V. L. Indenbom, E. B. Loginov, and M. A. Osipov, *Sov. Phys. Crystallogr.* **26**(6), Nov.-Dec. 1981.
- [5] Wenhui Ma, *Phys. Scr.* **T129** (2007) 180-183.
- [6] E. F. Bertaut, D. Fruchart, J. P. Bouchaud, and R. Fruchart, *Solid State Commun.* **6**, 251 (1968).
- [7] P. Lukashev, R. Sabirianov, and K. Belashchenko, *Phys. Rev. B* **78**, 184414 (2008).
- [8] P. Blöchl, "Projector augmented-wave method", *Phys. Rev. B* **1994**, 50, 17953.

- [9] G. Kresse and D. Joubert, "From ultrasoft pseudopotentials to the projector augmented-wave method", Phys. Rev. B **1999**, 59, 1758.
- [10] J.P. Perdew, K. Burke, and M. Ernzerhof, Phys. Rev. Lett. **1996**, 77, 3865.
- [11] P.E. Blöchl, O. Jepsen, O.K. Andersen, Improved tetrahedron method for Brillouin-zone integrations. Phys. Rev. B **1994**, 49, 16223.